Vol. 591: 167–183, 2018
https://doi.org/10.3354/meps12255

MARINE ECOLOGY PROGRESS SERIES
Mar Ecol Prog Ser

Published March 19[§]

Contribution to the Theme Section 'Jellyfish bloom research: advances and challenges'

Modeling population dynamics of scyphozoan jellyfish (*Aurelia* spp.) in the Gulf of Mexico

Natasha Henschke[1,*], Charles A. Stock[2], Jorge L. Sarmiento[1]

[1]Program in Atmospheric and Oceanic Sciences, Princeton University, Princeton, NJ 08540, USA
[2]Geophysical Fluid Dynamics Laboratory, NOAA, 201 Forrestal Road, Princeton, NJ 08540, USA

ABSTRACT: To gain understanding and predict how jellyfish populations will respond to anthropogenic changes, we first need to understand the factors that influence the distribution and abundance of current and historical populations. Hence, we have developed the first bioenergetics-based population model for the ubiquitous jellyfish *Aurelia* spp. that incorporates both benthic and pelagic life history stages. This model tracks cohorts of both life stages with temperature- and/or consumption-driven relationships for growth, reproduction and mortality. We present an initial model application to test hypotheses for the environmental factors that control the initiation of strobilation and inter-annual variability in bloom timing and magnitude in Gulf of Mexico jellyfish populations between 1982 and 2007. To recreate the autumnal blooms of *Aurelia* spp. in the Gulf of Mexico, strobilation must commence while zooplankton biomass is increasing after the annual minimum. Under this scenario, the model simulated seasonal and inter-annual variability of *Aurelia* spp. biomass that corresponded well with observations. Markedly larger blooms in anomalously warm, high zooplankton years resulted from enhanced ephyrae production compounded by enhanced medusa growth under these conditions. This model confirms the importance of the polyp-to-ephyrae transition in regulating jellyfish bloom magnitude and provides a mechanistic model framework which can examine how future jellyfish populations might respond to climate change.

KEY WORDS: Jellyfish · *Aurelia aurita* · Population modeling · Climate change

INTRODUCTION

Jellyfish (cnidarians and ctenophores) can occur in elevated concentrations (i.e. blooms) in coastal and shelf ecosystems. Two main bloom mechanisms are recognized: rapid population growth (true blooms) and advection/translocation of individuals (apparent blooms; Graham et al. 2001). Both types of blooms are a natural phenomenon, yet as true blooms tend to occur seasonally, their timing is often relatively predictable compared to apparent blooms (Graham et al. 2001, Gershwin et al. 2014). Large blooms of jellyfish can have deleterious consequences, including loss of tourist revenue at beaches (Purcell et al. 2007) and reduction in commercial fish catch through competition, predation and burst fishing nets (Lynam et al. 2006). While several jellyfish species can form blooms, many scyphozoan jellyfish are well documented for their ability to form large blooms, as they are predominantly coastal and have a life cycle that alternates between sexual medusoid and asexual, benthic polypoid reproduction (Hamner & Dawson 2009). Throughout the remainder of this study, we will only be considering scyphozoan jellyfish blooms that are the result of population dynamics (true blooms).

The benthic polypoid phase is an important perennial stage that can survive for months at low food concentrations (Lucas et al. 2012) and allows jellyfish populations to survive when recruitment to the sexual medusoid phase fails (Willcox et al. 2008). The general paradigm is that the scyphozoan life cycle

*Corresponding author: natashahenschke@gmail.com
[§]Advance View was available online October 6, 2017

is metagenic and includes an obligatory alternation between polyp and medusa stages. Polyps reproduce asexually by several modes: by producing resting stages called podocysts, budding new polyps and/or strobilating to produce ephyrae (Arai 1997). Ephyrae develop into medusae and, once mature, reproduce sexually and release planula larvae which settle and metamorphose into polyps (Arai 1997). Jellyfish bloom magnitude reflects the success of the polyp stage in producing ephyrae and subsequent survival of the medusae. However, compared to medusae, very little is known about the polyp stage. Few ecological studies exist for polyps *in situ* as they are very small (<5 mm; Ishii & Watanabe 2003) and are difficult to locate and identify accurately to species level (Pitt 2000). *Aurelia* spp. polyps have been found attached to the side or underside of marinas, pylons, cement breakwaters, floating piers and iron wrecks at shallow depths (<14 m) and across a wide range of temperature (5–20°C) and salinity conditions (21–34; Miyake et al. 2002, Willcox et al. 2008, Purcell et al. 2009, Di Camillo et al. 2010, Ishii & Katsukoshi 2010). Laboratory-based studies on polyps have identified that some blooming scyphozoan jellyfish species (e.g. *Aurelia* spp., *Chrysaora melanaster* and *Nemopilema nomurai*) are expected to benefit from climate change through increased growth rates, asexual reproduction rates and/or feeding rates as a response to increasing temperature (Purcell et al. 2009, 2012). However, due to the paucity of information on *in situ* polyp populations, it is difficult to accurately forecast and predict the magnitude of jellyfish blooms, and previous research on jellyfish bloom dynamics fails to include this important life-history stage.

To more holistically understand the factors that determine jellyfish blooms and build predictive capacity, we have developed a size-structured population model for the ubiquitous moon jellyfish (*Aurelia* spp.) that incorporates both benthic and pelagic life-history stages. *Aurelia* spp. are cosmopolitan generalists (Dawson & Martin 2001), occurring circumglobally between 70° N and 40° S (Möller 1980) in dense blooms of up to 300 ind. m^{-3} (Olesen et al. 1994). While many ecological responses are likely to be shared among different populations of *Aurelia* spp., there are clear population-specific responses to environmental changes which indicate that different *Aurelia* spp. populations have locally adapted to their environment (Pascual et al. 2015). Therefore, in this study we consider the local population of *Aurelia* spp. from the northern Gulf of Mexico. The Gulf of Mexico is a productive subtropical ecosystem that supports biological diversity and large fisheries (Muller-Karger et al. 2015). In the northern Gulf of Mexico, *Aurelia* spp. bloom regularly in autumn (October–November) in shallow waters (<40 m) and have been sampled yearly since 1982 (Robinson & Graham 2013), making this system a valuable case study for model comparison.

This model tracks cohorts of individuals using temperature- and/or consumption-driven relationships for size-specific growth, reproduction and mortality rates. As a result, this model can explore population dynamics during the development and demise of a jellyfish bloom across varying environmental conditions, and quantitatively test bloom initiation and development hypotheses. The timing of strobilation of ephyrae from polyps to form new medusae is thought to be a major determinant of the success of jellyfish blooms. Several hypotheses exist for environmental cues for strobilation, including timing with the annual minimum in light, temperature, salinity and/or food supply (Willcox et al. 2008, Purcell et al. 2009). The general motivation is thought to be timing releases to maximize coincidence between medusa cohorts and favorable conditions for growth and survival. We considered 3 variants in this study and assessed them relative to their ability to explain observed bloom patterns in the Gulf of Mexico: Hypothesis 1 (H_1)—strobilation is initiated at the annual temperature minimum; H_2—strobilation is initiated at the annual zooplankton minimum; and H_3—strobilation is initiated during the annual increase in zooplankton biomass. During hypothesis testing, we considered the sensitivity of simulated blooms to all model parameters. We then examined the biophysical factors affecting the timing and extent of polyp and ephyrae production in the Gulf of Mexico, as these factors are highly uncertain but strongly influence medusa biomass (Robinson & Graham 2013).

METHODS

We developed a discrete-time, size-structured scyphozoan jellyfish population model, based on Gulf of Mexico populations of moon jellyfish *Aurelia* spp. The model tracks cohorts of individuals and their size at a daily time step. Each cohort represents a group of individuals that are born at the same time, with the assumption that all individuals within the cohort are the same size. Within a year, depending on the rate of reproduction (for both polyps and medusa), there may be several cohorts of differing size coexisting from the same generation. The model

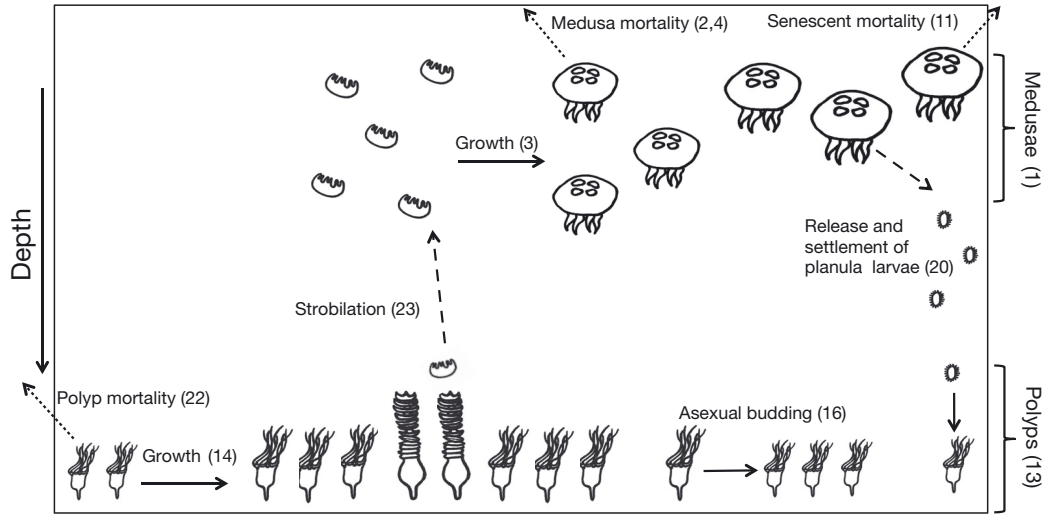

Fig. 1. Scyphozoan jellyfish model schematic. The model begins with a pre-existing polyp population and zero medusae. Polyp mortality is dependent on predation, and growth is dependent on consumption. Strobilation is initiated as a function of temperature, and the amount and rate of release of ephyrae is dependent on temperature, zooplankton biomass and polyp size. Polyps asexually bud when temperatures increase, and the number of buds produced is dependent on temperature, zooplankton biomass and polyp density. Medusae will grow relative to temperature and zooplankton biomass, and mortality is dependent on zooplankton biomass (i.e. starvation) and predation. The amount of planula larvae released is dependent on medusa size. Once sexually mature, medusae will rapidly senesce. Planula larvae settle as polyps, with settlement rates dependent on polyp density. Dashed lines represent a shift in generations, dotted lines represent mortality loss, and solid lines represent growth or reproduction. Numbers in parentheses refer to the equations in the 'Methods'

uses 6 state variables to simulate the processes depicted in Fig. 1: density of polyps (P_N, polyps m^{-2}), polyp size expressed as carbon biomass (P_C, µg C polyp^{-1}), number of actively feeding medusae (M_N, medusae m^{-3}), medusa size expressed as carbon biomass (M_C, mg C medusa^{-1}), number of senescent post-reproductive medusae (S_N, senescent medusae m^{-3}) and senescent medusa size expressed as carbon biomass (S_C, mg C senescent medusa^{-1}). Both abundance and biomass are tracked throughout the model to be consistent with methods used in observations: abundance for polyps and abundance or biomass for medusae. Temperature and zooplankton biomass were used as the external drivers in this model, given their known association with jellyfish feeding, physiology and life-cycle transitions (Lucas 2001). Temperature- and zooplankton-dependent relationships are derived from empirical data covering a range of temperate and tropical environments that encompass the same environmental conditions expected to occur in

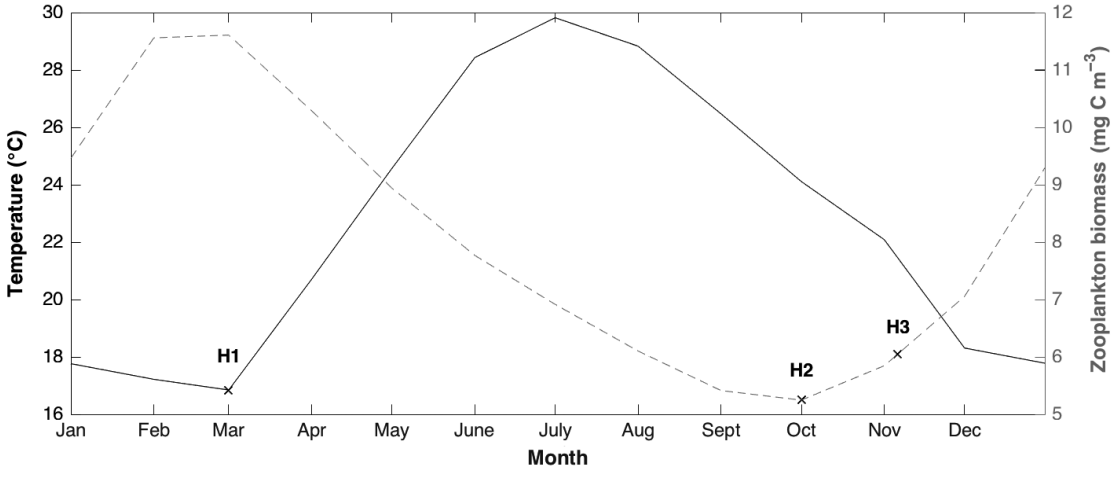

Fig. 2. Long-term (1982–2007) mean monthly temperature and zooplankton biomass for the sampling area. H_1, H_2 and H_3 indicate the starting temperatures for the initiation of strobilation for each hypothesis (see 'Introduction' and 'Methods' for details of the hypotheses)

the Gulf of Mexico (Fig. 2). While other environmental variables such as salinity (Holst & Jarms 2010) and light (Liu et al. 2009) have been shown to influence asexual reproduction rates in polyps, these effects generally occur under extreme conditions that are unlikely to happen in the northern Gulf of Mexico. Thus they were not considered as external drivers in this initial model framework.

Our objective was to establish a baseline structure for a scyphozoan jellyfish population model with parameters chosen to best mimic *Aurelia* spp. Because jellyfish population dynamics are often difficult to observe, each aspect of the life cycle has significant uncertainty. The model is thus intended as an initial mechanistic framework for exploring hypotheses for the factors controlling scyphozoan jellyfish life cycle dynamics and the emergent implications of these hypotheses on jellyfish distribution and abundance. The process of formulating the model forced us to confront numerous poorly constrained processes, and subsequent sensitivity studies revealed which of those processes mapped strongly onto observed blooms.

Medusa dynamics

The time (t) evolution of the number of active medusae in each cohort is governed by:

$$\frac{dM_N}{dt} = strob - pred_M - starve - repro \quad (1)$$

where *strob* is the production of ephyrae (larval medusae) strobilated from polyps, $pred_M$ (predation) and *starve* (starvation) are mortality losses of medusae, and *repro* are losses of post-reproductive medusae to senescence. All sources and sinks in Eq. (1) are tracked as medusae m^{-3} d^{-1}.

Medusa predation losses are assumed to be density-dependent:

$$pred_M = m_M \cdot \sum M_N \cdot M_N \quad (2)$$

where m_M (d^{-1} [medusae m^{-3}]$^{-1}$) is a scaling coefficient set such that medusa mortality reaches ~0.05 d^{-1} at high medusa densities (Table 1). The summation in Eq. (2) indicates that the predation rates increase in proportion to the medusa density summed over all cohorts. The density-dependence of predation mortality mirrors findings for mesozooplankton (e.g. Ohman et al. 2002) and reflects an assumption that the biomass of unresolved predators scales in proportion to the biomass of unresolved prey (Steele & Henderson 1993). Such aggregation is consistent with observations of foraging behaviors of sea turtles and other obligate predators of gelatinous species (Houghton et al. 2006). The scaling coefficient was chosen to be comparable in magnitude to the findings of Oviatt & Kremer (1977) during blooms of the ctenophore *Mnemiopsis leidyi* where predation reached a maximum of 0.05 d^{-1} at population biomasses of ~10 mg C m^{-3}. This biomass value is equivalent to mean population biomass calculated from observations in the Gulf of Mexico when using mean abundance (0.02 ind. m^{-3}) and assuming a large medusa size (200 mm).

The growth of the medusae (mg C medusa^{-1} d^{-1}) in each cohort is determined by the balance of energy intake minus respiration:

Table 1. Parameter values used in the model simulation and the relevant equation(s) in the 'Methods' and Fig. 3. Parameters in **bold** were included in the sensitivity analysis. Sources are 1: Oviatt & Kremer (1977); 2: Hamner & Jenssen (1974); 3: Schneider (1989); 4: Ishii & Bamstedt (1998); 5: Fu et al. (2014); 6: Møller & Riisgård (2007a); 7: Gatz et al. (1973); 8: Kamiyama (2011); 9: Willcox et al. (2008); 10: Liu et al. (2009); 11: Purcell (2007); 12: Purcell et al. (2012); 13: Pascual et al. (2015); 14: Holst (2012); BG: best guess

Parameter	Equation	Description	Value	Source
$\boldsymbol{m_M}$	2	Predation mortality	0.002	1
DG	3, 12	Medusa shrinkage	0.06	2
γ	3, 14	Assimilation efficiency	0.8	3
$\boldsymbol{m_s}$	4, 11	Starvation/senescent mortality	0.1	4, 5
a, *b*	7	Medusa clearance rate	3.2×10^{-5}, 2.3	6
c, d, f, g	8	Temperature-dependent pulsation	0.295, 23, 11, 0.0633	7
PK	13	Polyp-carrying capacity	20–500	BG
h, j	18	Polyp ingestion	1.031, 0.2	8
$\boldsymbol{m_P}$	22	Polyp mortality	0.002	9
k, l	23	Temperature-dependent ephyra production (T ≤ 20°C)	2.5543, 6.9988	10–14
n, o	23	Fraction of polyps strobilating (T ≤ 20°C)	4.2143, 3.9105	10–14
k, l	23	Temperature-dependent ephyra production (T > 20°C)	−0.3323, 16.467	10–14
n, o	23	Fraction of polyps strobilating (T > 20°C)	1.9, 13.444	10–14

$$\frac{dM_C}{dt} = (\gamma I_M - resp_M) \cdot DG \quad (3)$$

where γ is the assimilation efficiency (dimensionless), I_M is the ingestion rate of medusae (mg C medusa^{-1} d^{-1}), $resp_M$ is the respiration rate (mg C medusa^{-1} d^{-1}), and DG is the shrinkage rate (d^{-1}). If medusae are starved, they will shrink with a first-order rate constant equivalent to 0.006 d^{-1} (Hamner & Jenssen 1974). The assimilation efficiency was set to 0.8 (Schneider 1989), and individual growth cannot exceed maximum observed values (G_{max} = 0.24 d^{-1}; Møller & Riisgård 2007b).

Starvation occurs if respiration exceeds ingestion (i.e. $resp_M > I_M$) and is modeled using a first-order decay rate based on empirical data:

$$starve = m_s \cdot M_N \quad (4)$$

where starvation mortality (m_s) is set to 0.1 d^{-1} such that starvation reaches 100% after 50 d (Ishii & Bamstedt 1998).

Medusa respiration rate (mg C medusa^{-1} d^{-1}; Fig. S1 in the Supplement at www.int-res.com/articles/suppl/m591p167_supp.pdf) is temperature-dependent and calculated from the empirically determined allometric relationship of Han et al. (2012):

$$resp_M = C:O \cdot 0.13 \cdot 2.62^{\frac{T-20}{10}} \cdot \left(\frac{M_C}{C:WW}\right)^{0.93} \quad (5)$$

where $C:O$ is the conversion between mg C and ml O_2 (0.46:1) and $C:WW$ is the carbon to wet weight conversion (0.13:100; Uye & Shimauchi 2005).

Medusa ingestion was modeled using a Type I Holling functional response (Holling 1966) to observed mesozooplankton biomass (Z, mg C m^{-3}):

$$I = \alpha_M Z \quad (6)$$

where α_M is the clearance rate per medusa (m^3 medusa^{-1} d^{-1}; Møller & Riisgård 2007a):

$$\alpha_M = a \cdot L_M{}^b \cdot Pulse \quad (7)$$

where a and b are constants (Fig. S1). $Pulse$ is a factor accounting for the deviation of maximum pulsation rate with temperature and is based on the difference between the current temperature (T) and that at which maximum pulsation rate occurs (Gatz et al. 1973):

$$Pulse = c \cdot \left(1 - \left(\frac{T-d}{f}\right)^2\right) \cdot e^{g \cdot (T-d)} \quad (8)$$

where c, d, f and g are constants (Table 1). $Pulse$ is fit such that maximum pulsation rate ($Pulse_{max}$) occurs at 26°C before dropping off on either side of this maximum (Fig. S1). $Pulse_{max}$ was determined to occur at 26°C based on trends observed across different subtropical and tropical scyphozoan species, whereby the peak pulsation rates occurred at the 75th percentile of ambient temperature range (Gatz et al. 1973). As medusae pulsate to create a feeding current, this relationship suggests that at temperatures on either side of the optimum, pulsation rate would be lowered and hence clearance rate would be reduced in a similar fashion.

Medusa reproduction and senescence are functions of bell diameter (L_M, cm), which is calculated from carbon biomass using the empirical relationship of Uye & Shimauchi (2005):

$$L_M = \left(\frac{M_C}{C:WW \cdot 0.0748}\right)^{\frac{1}{2.86}} \quad (9)$$

Medusa losses due to reproduction and senescence ($repro$, medusae m^{-3} d^{-1}) occur following the onset of sexual maturity. It is unknown how sexual maturity in females is initiated; however, it is believed to be a combination of size and temperature in temperate environments (Lucas 2001). As environmental conditions in the Gulf of Mexico are more tropical, here we assumed that size is a proxy of sexual maturity. Once reproduction is initiated in females, it has been observed that the rest of the medusa population becomes sexually mature, regardless of size (Lucas 2001). Hence, a logistic curve was used to represent the proportion of females reproducing per day, where 50% of available females will reproduce at the median size for observed reproductive females (100 mm; Lucas 2001):

$$repro = \frac{1}{1 + e^{-0.1(L_M - 100)}} \cdot M_N \quad (10)$$

The slope (–0.1) spreads the majority of reproduction over a ~2 d to 2 wk window depending on medusa growth rates (Fig. S1).

After reproduction, senescence in both male and female medusae is rapid due to increased predation and starvation as they often shed their feeding organs with their reproductive organs (Spangenberg 1965, Möller 1980). Here we assumed that senescent mortality rates mirror those of starving medusae, set to 0.1 d^{-1} such that starvation reaches 100% after 50 d (Ishii & Bamstedt 1998). Senescent medusae (S_N; senescent medusa m^{-3}) of size S_C (mg C senescent medusa^{-1}) decay with a first-order rate constant m_s, equivalent to starving medusae:

$$\frac{dS_N}{dt} = repro - m_s S_N \quad (11)$$

and shrink with a first-order rate constant DG:

$$\frac{dS_C}{dt} = DG \cdot S_C \quad (12)$$

Polyp dynamics

The change in the number of polyps (P_N, polyps m^{-2} d^{-1}) arises from additions via planula larvae produced during medusa reproduction (*plan*), asexual budding of existing polyps (*bud*) and losses due to predation ($pred_P$). The ability of the source terms to augment the polyp population, however, is limited by the carrying capacity (*PK*, polyps m^{-2}) of the sediment substrate (Coyne 1973, Gröndahl 1988, Watanabe & Ishii 2001). We used a Verhulst equation to represent the carrying capacity effect:

$$\frac{dP_N}{dt} = (bud + plan)\cdot\left(1-\frac{P_N}{PK}\right) - pred_P \quad (13)$$

where all sources and sinks of polyps are tracked in polyps m^{-2} d^{-1}. The central assumption of the equation is that the rate of increase in polyp abundance is proportional to the supply of new polyps and the space to accommodate them. While polyps are also able to asexually produce podocysts, which are capable of then producing fully active polyps, few quantitative data are available on rates of podocyst production (Arai 2009), and it appears to mainly occur at much lower frequencies than bud formation (1%; Han & Uye 2010). Regardless, the formation of new polyps via budding or podocyst formation will both result in increases in the polyp population. In order to simply this process, and reduce the amount of assumptions related to polyp community dynamics, here we assumed that any addition of new polyps through asexual reproduction is encompassed in the *bud* term.

Increase in polyp size (P_C; µg C $polyp^{-1}$) is determined by the balance of energy intake minus respiration and the partitioning of energy between growth, budding and strobilation (Han & Uye 2010):

$$\frac{dP_C}{dt} = \varepsilon\cdot(\gamma I_P - resp_P) - strob\cdot C:Ephyra \quad (14)$$

where ε is the proportion of energy used for somatic growth (dimensionless), γ is the assimilation efficiency (dimensionless), I_P is the ingestion rate of polyps (µg C $polyp^{-1}$ d^{-1}), $resp_P$ is the respiration rate (µg C $polyp^{-1}$ d^{-1}), and *C*:*Ephyra* is the carbon content of a recently released ephyra (22 µg C, assuming ephyrae are released at 6 mm; Spangenberg 1965).

Polyps grow to a maximum size of 5 mm or 162 µg C (Ishii & Watanabe 2003), at which point all energy is presumed to be allocated to budding. The partition of energy surpluses between polyp growth and budding below maximum size, however, is uncertain. Empirical evidence from Han & Uye (2010) suggests a temperature-dependent linear tradeoff between the amounts of energy used for somatic growth and asexual reproduction, such that polyps will favor somatic growth at lower temperatures and asexual reproduction at higher temperatures. The lowest polyp growth and highest rate of budding were observed at 28°C (Han & Uye 2010). Hence the proportion of energy used for somatic growth (ε) is calculated from:

$$\varepsilon = max\left(1-\frac{T}{28},0\right) \quad (15)$$

where if the current temperature (T) exceeds 28°C, it is assumed that ε = 0.

The production of new polyps through budding (i.e. *bud* in Eq. 13) is then dependent on the fraction of energy not used for somatic growth:

$$bud = \frac{(1-\varepsilon)\cdot(\gamma I_P - resp_P)\cdot P_N}{C:Polyp} \quad (16)$$

where *C*:*Polyp* is the carbon content of a small-sized polyp (1 mm or 38 µg C; Kamiyama 2011) to give a flux of polyps due to budding in polyps m^{-2} d^{-1}. As budding usually occurs in summer (Lucas et al. 2012), in this model we have restricted budding to the period of time around the annual temperature maximum (T_{max}) ± 45 d. The surplus of energy not used for growth or budding (*store*; µg C d^{-1}) (i.e. when polyps reach their maximum size, or budding has completed) is stored for strobilation and contributes to the amount of ephyrae released per polyp:

$$\begin{aligned} store &= \varepsilon\cdot(\gamma I_P - resp_P) && \text{if } P_C \geq 162 \text{ µg C} \\ store &= (1-\varepsilon)\cdot(\gamma I_P - resp_P) && \text{if day} \neq \text{day}_{T_{max}} \pm 45 \end{aligned} \quad (17)$$

Polyp ingestion is modeled as a Type II Holling response (Kamiyama 2011):

$$I_P = \frac{h\cdot Z}{j+Z} \quad (18)$$

where *h* and *j* are constants set so that ingestion saturates at 8 µg C $polyp^{-1}$ d^{-1} at a prey density of ~500 mg C m^{-3} (Kamiyama 2011). Polyp respiration (Fig. S1) is calculated from Gambill & Peck (2014):

$$resp_P = C:O\cdot 5.463\cdot\left(\frac{P_C}{C:DW}+4.1484\right) \quad (19)$$

where *C:O* is the carbon to oxygen conversion (1:0.46; Uye & Shimauchi 2005) and *C:DW* is the carbon to dry weight conversion (1:223; Kamiyama 2011). Respiration rates are based on polyps at 15°C and do not include temperature-dependent effects. Polyp respiration did not significantly differ at temperatures above 15°C and was low at tempera-

tures below 15°C (Gambill & Peck 2014). As water temperatures in the Gulf of Mexico are >15°C, including a temperature dependence on polyp respiration will not improve the model in its current form. However, more empirical evidence may be necessary to determine how polyps respire at low temperatures, particularly if applying the model to cooler environments.

The number of settling planula larvae from each medusa cohort is calculated as:

$$plan = repro \cdot 0.5 \cdot PL \quad (20)$$

where $repro \cdot 0.5$ is the number females undergoing reproduction per day (sex ratios are generally 1:1; Lucas 2001). While the mortality of planula larvae in the water column is expected to be high (Lucas 2001), here we assumed that alternative sources of planulae mortality are captured by the carrying capacity (*PK*; Eq. 13) of the sediment substrate. *PL* is the abundance of planula larvae (larvae medusa^{-1} m^{-3}; Fig. S1) released per reproductive female, which depends on medusa size as described by Lucas (1996):

$$PL = \left(\frac{M_C}{C:WW}\right) \cdot 267 + 247 \quad \text{if } M_C > 0 \quad (21)$$

These are integrated over depth to provide the total source of larvae to the sediment.

Polyps are perennial, with low mortality rates from competition for space (i.e. density-dependent mortality during settlement and budding captured by the Verhulst equation) and predation. Unlike the medusa stage, polyps do not have known specialized predators. Predation and other sources of mortality are rather thought to be incidental losses to more generalist benthic foragers and sediment disturbance. As a first approximation, we thus modeled polyp predation mortality with a low background density-independent mortality rate ($pred_p$):

$$pred_P = m_P P_N \quad (22)$$

where we set m_p to allow for ~50% turnover in the polyp biomass per year (i.e. 0.002 d^{-1}).

Polyps asexually produce ephyrae through strobilation. In this model, we assumed that the first cohort of ephyrae is released at the initiation of strobilation. The amount of ephyrae released from each polyp and the fraction of polyps strobilating increases with increasing temperature and increasing polyp size:

$$strob = E_{\max} \cdot S_T \cdot f_T \cdot P_N \quad (23)$$

where $E_{\max}$ is the proportional maximum number of ephyrae a polyp can produce, assuming that ephyrae production never exceeds 45 ind. polyp^{-1} d^{-1} (Purcell 2007). This is scaled by empirically determined temperature dependencies of the strobilation rate (S_T, Fig. 3a) and the fraction of strobilating polyps (f_T, Fig. 3b). $E_{\max}$ is dependent on the size of the polyp and the amount of surplus carbon that the polyp community stored since the last strobilation event:

$$E_{max} = \min\left(1, \frac{P_C + store}{C:Ephyra \cdot 45}\right) \quad (24)$$

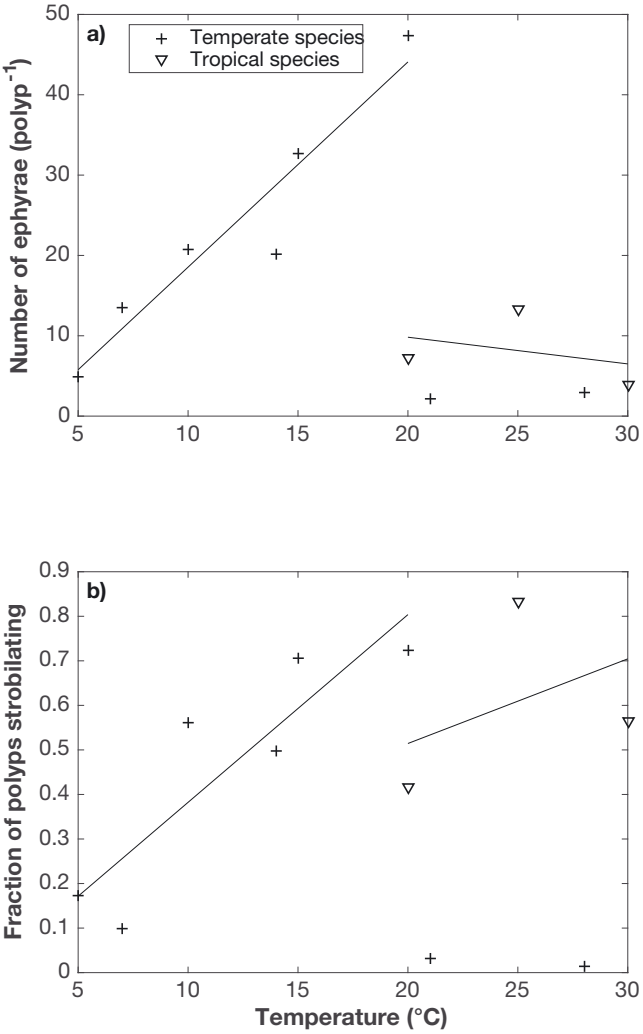

Fig. 3. Temperature-dependent relationships used to determine (a) the number of ephyrae produced per polyp and (b) the fraction of polyps strobilating. Data points are based on empirical data from Liu et al. (2009), Holst (2012), Pascual et al. (2015), Purcell (2007) and Purcell et al. (2012). Piecewise linear regressions were used to determine temperature-dependent relationships, with temperate and tropical species analyzed separately on either side of 20°C ($S_T = k \times Temp + l$; $f_T = n \times Temp + o$; see Eq. 23 and Table 1)

Strobilation hypothesis testing

The strobilation dynamics described earlier only apply once strobilation has been initiated by the polyp population. The 3 strobilation hypotheses we considered in this study are as follows.

H_1: Strobilation is initiated at the annual temperature minimum. Although no environmental variable has been singled out as the main regulator, the majority of authors agree that strobilation generally follows a reduction in temperature (Lucas 2001). Correspondingly, recent molecular evidence suggests that strobilation is initiated by a temperature-sensitive 'timer,' whereby *Aurelia* spp. polyps can distinguish between prolonged periods of cooler water during winter from short-term fluctuations to ensure strobilation is initiated during the correct season (Fuchs et al. 2014). The first hypothesis we consider is strobilation is initiated at the annual temperature minimum (i.e. after a prolonged period of cooling; Fig. 2).

In situ polyp populations have also been observed to strobilate during or after the annual minima in food supply (Willcox et al. 2008). There is strong seasonality in sea surface temperature (SST), net primary production (NPP) and mixed layer depth (MLD) in the Gulf of Mexico. NPP climatology peaks in productivity in February, during the SST minima and MLD maxima, and declines as SST increases and MLD becomes more shallow before reaching a minimum in September/October (Muller-Karger et al. 2015). Thus, since seasonal trends in zooplankton biomass generally correspond with seasonal temperature trends, and assuming the presence of a temperature-sensitive strobilation timer (Fuchs et al. 2014), we considered 2 additional prey-motivated alternative temperature cues:

H_2: Strobilation is initiated at the temperature that corresponds to the annual zooplankton minimum. The annual zooplankton minimum in the Gulf of Mexico based on long-term (1982–2007) mean values (Fig. 2) occurs in late September, after the summer peak in annual temperature once temperature has declined to ≈26°C. Thus, for this hypothesis we assumed that strobilation is initiated at 26°C.

H_3: Strobilation is initiated at the temperature that corresponds to the seasonal increase in zooplankton. This hypothesis assumes that strobilation is initiated during the annual increase in zooplankton biomass. We thus assumed that strobilation tends to begin when the zooplankton population has reached its median value following the autumn minimum. This generally corresponds to a maximum rate of increase and, climatologically, occurs in late October/early November at temperatures ~21°C. For this hypothesis, strobilation is initiated when temperature is equal to 21°C.

Aurelia spp. observations

Jellyfish biomass observations were estimated from fisheries-independent groundfish and shrimp trawl surveys collected by the Southeast Area Monitoring and Assessment Program (SEAMAP). SEAMAP is managed by the National Oceanic and Atmospheric Administration National Marine Fisheries Service and the Gulf States Marine Fisheries Commission. SEAMAP data was obtained through the publicly accessible Jellyfish Database Initiative (http://jedi.nceas.ucsb.edu; accessed on 09/15/2015; Lucas et al. 2014). The SEAMAP sampling area extends from Alabama to Texas, although for this study samples

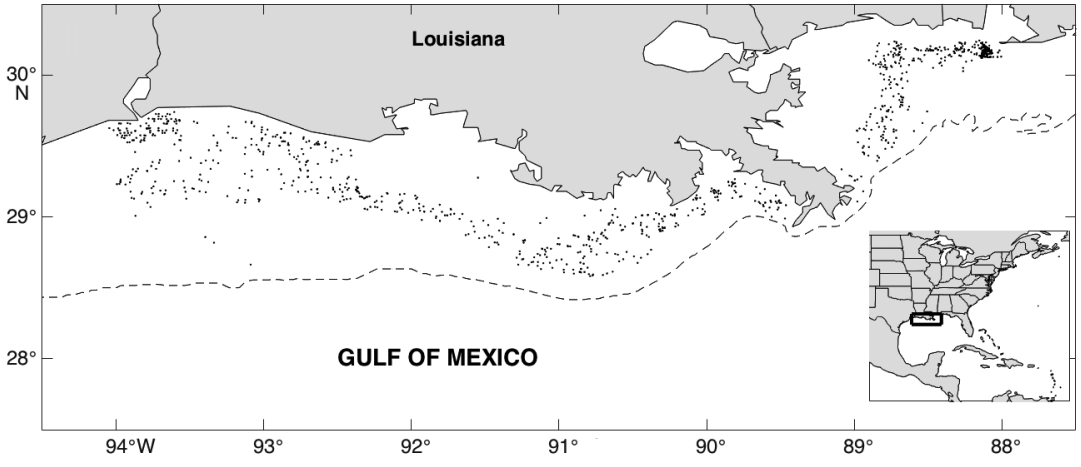

Fig. 4. SEAMAP sampling locations in the northern Gulf of Mexico. Dashed line indicates the 40 m isobath

were restricted to areas off Louisiana (Fig. 4) to be consistent with previous studies examining long-term trends in jellyfish biomass in the area (Graham 2001, Robinson & Graham 2013). Jellyfish surveys are conducted twice annually generally during summer (May–July) and autumn (October–November). The majority of jellyfish collections were made with a 12 m wide benthic shrimp trawl with a nominal mesh size of 3.8 cm, so it was assumed that only jellyfish individuals >5 cm were retained, and jellyfish only entered the nets on the oblique tow during deployment and recovery (Robinson & Graham 2013).

Temperature and zooplankton biomass data that were sampled in conjunction with SEAMAP were averaged across the whole sampling area and linearly interpolated into daily increments to match the time step of the model. Temperature and zooplankton data were sampled more frequently (i.e. several times a month) than jellyfish biomass, as all vessels participating in the program were equipped to measure environmental data. Mesozooplankton biomass in this application is drawn from a range of net types: Bongo nets, Tucker trawls and Neuston nets, ranging in mesh from 202 to 946 µm, with the majority of sampling (97 %) undertaken by a 333 µm mesh Bongo net (for full details of net types see www.st.nmfs.noaa.gov/copepod/data/us-05201/html_src/methods.html).

Model simulations

Simulations are done in an idealized 1 m^2 × 20 m box to represent the euphotic zone and median depth within the SEAMAP sampling area. To compare against the whole SEAMAP sampling area, we assumed that once released, ephyrae and medusae are evenly dispersed in the water column.

The northern Gulf of Mexico shelf encompasses a large area of hard substrate suitable for polyp settlement, both natural (oyster reef) and artificial (oil and gas rigs), particularly around the Louisiana shelf (Graham 2001) near the SEAMAP sampling area (Fig. 4). The actual distribution and abundance of polyps in the Gulf of Mexico, however, is unknown, and observed polyp densities in other systems are highly variable. We thus start by considering a single characteristic polyp density for the region that will be calibrated for each strobilation hypothesis (see next section).

To compare model output with observed jellyfish biomass data, simulations were run for the 26 yr period corresponding to SEAMAP data trawls (1982–2007). The model simulation was first spun-up under climatological mean temperature and zooplankton biomass until the polyp and medusa communities reached a quasi steady-state before commencing the model simulations. While Fig. 1 displays the basic elements of the scyphozoan jellyfish life cycle, recent evidence suggests additional complexities that question this paradigm. For example, in certain species, individuals can bypass either the sexual or asexual phase of their life cycle; ephyrae have been developed directly from planula larvae, and polyps can be produced directly from juvenile medusae (Arai 1997, He et al. 2015). Additionally, it has been theorized that *Chrysaora plocamia* medusa may overwinter, which can result in a multi-modal as opposed to a metagenic life cycle (Ceh et al. 2015). While these processes have the potential to influence bloom dynamics, the limited extent of knowledge makes them difficult to include in a baseline parameterization. Thus, for a first approximation, here we assumed a metagenic life cycle, and that only 1 strobilation event occurs each year (Agassiz 1860). At each daily time step, medusa population biomass was calculated from the carbon biomass and abundance of medusae and senescent medusae individuals.

The timing, magnitude and inter-annual variability of the jellyfish bloom was used to assess the model and identify which strobilation hypothesis best matched the empirical data. Bloom timing was calculated based on seasonal means to overcome the lack of consistent monthly sampling in the observations. Winter (DJF) was ignored, as there were not enough observations to calculate an accurate seasonal mean (n = 2). The timing of the modeled bloom was determined as the season with the highest medusa biomass. Bloom magnitude was computed as the mean medusa biomass from the season with the largest medusa bloom. The model skill in assessing inter-annual variability in biomass was assessed by comparing the mean of all observed monthly biomass data to the mean of all of the corresponding monthly modeled biomass data in each year of the sampling period (1982–2007). ANOVAs were used to compare the magnitude of the jellyfish blooms from each hypothesis with the observed magnitude, and Pearson correlations were used to determine how well the modeled inter-annual variability matched trends in the observed data. Linear modeling was used to explore the environmental drivers of medusa biomass. Prior to analysis, possible outliers or collinearity were identified through graphical analysis (boxplots and pairwise scatter plots). No outliers were identified. Collinearity occurred between medusa growth rate

and temperature deviation from the 26°C optimum ($r = -0.68$, $p < 0.001$), and between zooplankton biomass 10 d prior to strobilation and zooplankton biomass at strobilation ($r = 0.94$, $p < 0.001$). Hence both growth rate and zooplankton biomass at strobilation were not included as factors in the linear model. Covariates that were included in the linear model were polyp abundance, temperature deviation from the optimum 30 d after strobilation and zooplankton biomass 10 d prior to strobilation. The 30 d temperature deviation from the optimum was used to indicate temperature conditions during the development of the medusa bloom, whereas the zooplankton biomass 10 d prior to strobilation was used to indicate the conditions prior to the bloom while polyps are storing carbon for strobilation.

Calibration and sensitivity analysis

In order to test the strobilation hypotheses described above, we must assess whether differences in model skill can be attributed to strobilation and not explained equally well by variations in other uncertain parameters. As noted above, the polyp-carrying capacity of the sediment substrate is poorly constrained, with *in situ* observations of polyp density ranging from 5 to 400 000 ind. m^{-2} (Miyake et al. 2002, Willcox et al. 2008, Purcell et al. 2009, Di Camillo et al. 2010, Ishii & Katsukoshi 2010). Hence, before testing the strobilation hypothesis, initial sensitivity tests for polyp-carrying capacity magnitudes spanning this range (5–400 000 ind. m^{-2}) were carried out. Varying polyp-carrying capacity across its uncertainty bounds varied mean bloom magnitude across years by a factor of 5 to 8, but had a negligible impact on bloom timing.

As a result of the large uncertainty in polyp-carrying capacity of the sediment substrate, any of the strobilation hypotheses above can match bloom magnitude after calibration of polyp-carrying capacity within its uncertainty bounds. Our approach for comparing hypotheses was thus to calibrate the polyp-carrying capacity for each hypothesized strobilation model to the mean observed bloom magnitude and distinguish the hypotheses based on the timing and inter-annual variability metrics (i.e. the seasonal peak of the bloom and the correlation with observed inter-annual variability in bloom magnitude). The robustness of differences in these skill metrics to uncertainty in other parameters was assessed with a Monte Carlo approach, where all of the parameters in Table 1 were randomly varied by ± 20% of their value until their variance stabilized (2000 model realizations).

RESULTS

All strobilation hypotheses were able to reproduce realistic bloom magnitudes, but the polyp-carrying capacity required to simulate medusa blooms in the same magnitude as observations varied across the different hypotheses (Table 2). H_1 required low polyp abundances (20 ind. m^{-2}) whereas H_2 and H_3 required higher abundances of polyps (100–500 ind. m^{-2}). The correct autumnal (SON) bloom timing was simulated when strobilation coincided with the zooplankton minimum (H_2) and median (H_3). By contrast, when strobilation was initiated at the minimum annual temperature (H_1), jellyfish blooms occurred in spring (MAM). Inter-annual variability of medusa biomass across the time series was only captured by H_3 ($r = 0.7$, $p < 0.001$). Differences in bloom timing and inter-annual variability among the hypothesis scenarios were robust to uncertainty in parameters other than when strobilation was initiated and polyp-carrying capacity (Fig. 5).

As H_3 reproduced the most realistic jellyfish bloom dynamics for the Gulf of Mexico, we diagnosed this simulation to gain insight into factors capable of explaining observed variations in jellyfish bloom magnitude in the Gulf of Mexico. Demographic characteristics of the polyp and medusa

Table 2. Seasonal bloom timing, bloom magnitude and inter-annual variation from simulation hypothesis testing and the polyp-carrying capacity that gave the best agreement with observed bloom magnitude. *Significant correlation at $p < 0.001$. H_1: temperature minimum; H_2: temperature corresponding with zooplankton minimum abundance; H_3: temperature corresponding with zooplankton median abundance; nd: no data; na: not applicable

	Observations	H_1	H_2	H_3
Polyp-carrying capacity (ind. m^{-2})	nd	20	100	500
Bloom timing (season)	Autumn (SON)	Spring (MAM)	Autumn (SON)	Autumn (SON)
Bloom magnitude (mg C m^{-3})	9.9 ± 14.3	9.2 ± 4.6	12.9 ± 4.2	12.4 ± 8.9
Inter-annual variation (correlation)	na	−0.17	0.25	0.7*

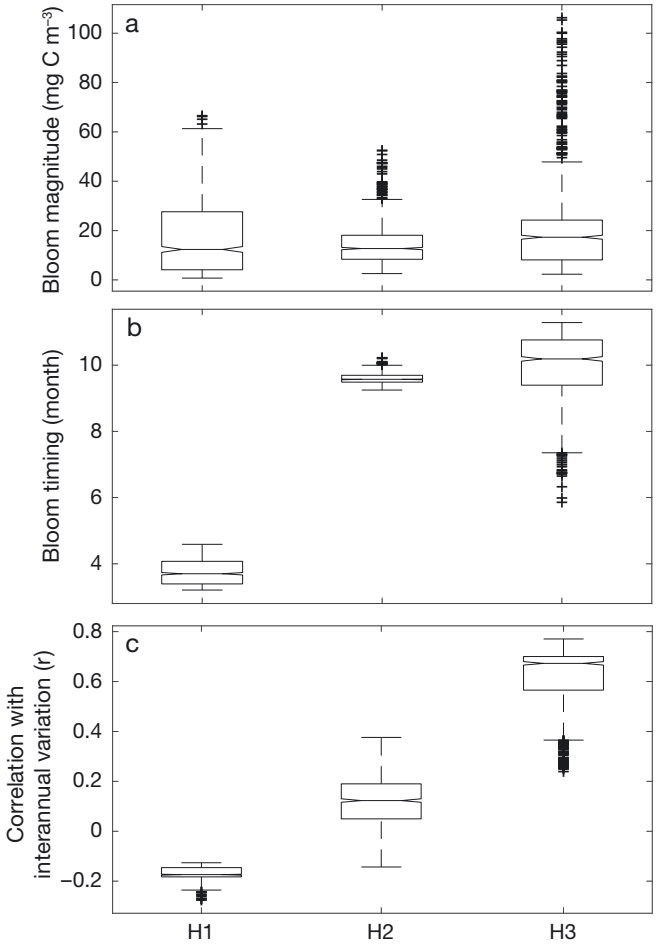

Fig. 5. Results from hypothesis testing showing the differences in (a) bloom magnitude, (b) bloom timing and (c) interannual variability in medusa biomass (correlation of model and observed bloom biomass over the 26 yr study period) across each hypothesis scenario (see 'Introduction' and 'Methods' for details of the hypotheses) when uncertain parameters are varied by ±20%. The central line of each box indicates the median, the edges indicate the 25th and 75th percentiles and the whiskers extend to the most extreme data points. Outliers are plotted using the '+' symbol

community simulated by the model corresponded well with ranges observed *in situ* (Table 3). Polyp abundance remained relatively stable, with an overall mean across the 26 yr period of 439 ± 3 ind. m^{-2} (Fig. 6a). Polyp abundance showed similar seasonal trends across the simulation, with regular peaks in abundance in summer after budding. Strobilation initiation date ranged from 13 October to 15 November. On average, 54% of the polyp population strobilated, releasing 10 ephyrae polyp^{-1}. Polyp abundance did not correlate significantly with medusa biomass ($p = 0.44$).

H_3 model simulations successfully reproduced the seasonal ($r = 0.61$, $p < 0.01$) and inter-annual cycles ($r = 0.7$, $p < 0.001$) of medusa biomass in the Gulf of Mexico (Fig. 6b, Table 2). Bloom longevity is calculated as the duration from the first day of ephyrae release until the demise of all medusa biomass from that year. Mean bloom longevity was 141 ± 1 d (Table 3). Medusa biomass varied across years, with an overall mean (excluding zero data) of 55 ± 47 mg C m^{-3} and peaked in late autumn to early winter (October to December). Mean bell diameter for the medusa population was 81 mm and reached a maximum size of 143 mm. When comparing the long-term trend (5 yr mean) in medusa biomass between model simulations and observations, both showed a similar trend of increasing biomass in the 1990s before a decrease in 2002 ($r = 0.94$, $p < 0.001$).

Linear modeling was undertaken to help identify the relationship between annual medusa biomass and select variables (Table 4). Variations in annual medusa biomass were strongly related to zooplankton biomass 10 d prior to strobilation and the deviation of temperature from the optimum (i.e. the temperature at which pulsation rate is maximized [$Pulse_{max}$]) 30 d after strobilation ($R^2 = 0.85$, $F = 69.5$, $p < 0.001$; Table 4).

A closer look at the composite blooms from large and small bloom years provides further insight into the mechanisms underlying relationships revealed by the linear modeling (Fig. 7). Large bloom years were characterized by relatively warm conditions with high zooplankton biomass anomalies during the months prior to the bloom (Fig. 7a,b). These conditions favored higher polyp abundance (Fig. 7c), but were particularly favorable for ephyrae production compared to small bloom years

Table 3. Demographic characteristics of *Aurelia* spp. polyp and medusa populations from the H_3 model simulation (see 'Introduction' and 'Methods' for details of the 3 hypotheses tested) and literature values. Sources are 1: Burke (1975); 2: Burke (1976); 3: Purcell et al. (2009); 4: Willcox et al. (2008); 5: Lucas et al. (2014); 6: Di Camillo et al. (2010); 7: Miyake et al. (2002); 8: Ishii & Katsukoshi (2010); 9: Phillips (1971)

Demographic characteristic	Modeled mean ± SD (range)	Literature range (source)
Swarm longevity (d)	141 ± 1 (139–145)	60–120 (1,2)
Ephyra released (ind. polyp^{-1})	10.4 ± 0.4 (9–14)	3–19 (3)
Fraction strobilating (%)	54 ± 0.08 (53.9–54.2)	13–82 (3,4)
Medusa biomass (mg C m^{-3})	55 ± 47 (0.2–198)	0.39–1177 (5)
Polyp abundance (ind. m^{-2})	439 ± 3 (338–501)	5–400000 (3,4,6,7,8)
Medusa size (mm)	81 ± 5 (10–143)	10–290 (9)

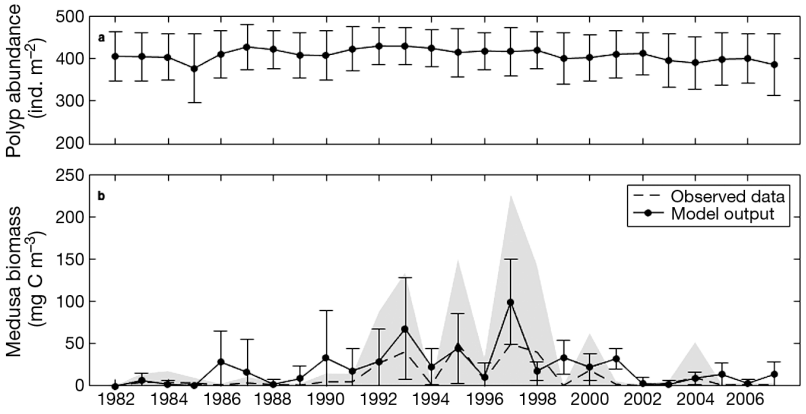

Fig. 6. Mean (±SD) inter-annual (a) polyp abundance and (b) medusa biomass simulated by the model (black circles) and observed from SEAMAP trawls (dashed line/grey shading)

Table 4. Linear model results for medusa biomass. Covariates include zooplankton biomass 10 d prior to strobilation and temperature deviation away from the optimum 30 d after strobilation. *Significant at $p < 0.001$

Coefficient	Estimate	SE	*t*	p
Intercept	141.141	19.848	7.111	3.04×10^{-7}*
Zooplankton biomass	1552.919	618.482	2.511	0.0195
Temperature deviation	−18.233	2.266	−8.047	3.87×10^{-8}*

(Fig. 7d). Ephyrae were released approximately 1 mo earlier in large bloom years and once in the water column, the persistence of warm conditions/high zooplankton biomass over the next month kept growth conditions closer to optimal for the larger ephyrae 'seed' (Fig. 7e). This combination of factors produced a multiplicative effect across life stages that led to a marked increase in medusa biomass during autumn (Fig. 7f).

DISCUSSION

This is the first size-structured scyphozoan population model that incorporates both polyp and medusa life history stages with temperature- and/or consumption-driven growth, reproduction and mortality rates. Existing jellyfish models, whether they are bioenergetics-based (Haraldsson et al. 2012), logistical (Melica et al. 2014) or statistical (Decker et al. 2007), only considered 1 life history stage. The first dynamic scyphozoan model that included both polyp and medusa life history stages incorporated temperature-dependent relationships, but ignored feeding and somatic growth (Xie et al. 2015). By incorporating feeding and somatic growth in our model, this model builds on previous jellyfish model frameworks such as that of Xie et al. (2015) by incorporating additional consumption-dependent terms such as starvation mortality and shrinkage, as well as including consumption requirements for the rate of ephyrae production. In this model, zooplankton biomass and temperature were sufficient drivers to create realistic seasonal and inter-annual population dynamics of *Aurelia* spp. in the Gulf of Mexico during 1982 to 2007. Initial sensitivity analyses identified that polyp-carrying capacity of the sediment substrate strongly influenced the mean magnitude of medusa blooms, whereas the timing of strobilation influenced bloom timing and inter-annual variations in medusa biomass. Large medusa bloom years appear to be the result of several factors compounding across scyphozoan life stages: increased polyp abundance, increased and earlier ephyrae production and increased ephyrae/medusa growth rates. This highlights the importance of polyp and ephyrae dynamics in regulating medusa populations, as well as the need to incorporate polyps into future analyses of jellyfish bloom dynamics.

Polyp community dynamics

It is difficult to assess the accuracy of our modeled polyp abundance, as the abundance and distribution of scyphozoan polyps in the Gulf of Mexico are unknown. Mean polyp abundance across each hypothesis simulation (20–500 ind. m^{-2}) fell within *in situ* observations of polyp abundance (5 to 400 000 ind. m^{-2}; Table 3) due to the large variation in polyp community abundance. *In situ* studies of polyp communities have been undertaken across locations with varying environmental conditions: Washington, USA (Purcell et al. 2009), Tasmania, Australia (Willcox et al. 2008), Tokyo Bay, Japan (Ishii & Katsukoshi 2010) and Ancona, Italy (Di Camillo et al. 2010). At each location, polyp abundance peaked in summer after budding and/or planulae recruitment, similar to our model simulations.

Each hypothesis simulation required a different polyp-carrying capacity to simulate medusa blooms of the same magnitude as the SEAMAP observations. This is likely due to the differences in temperature

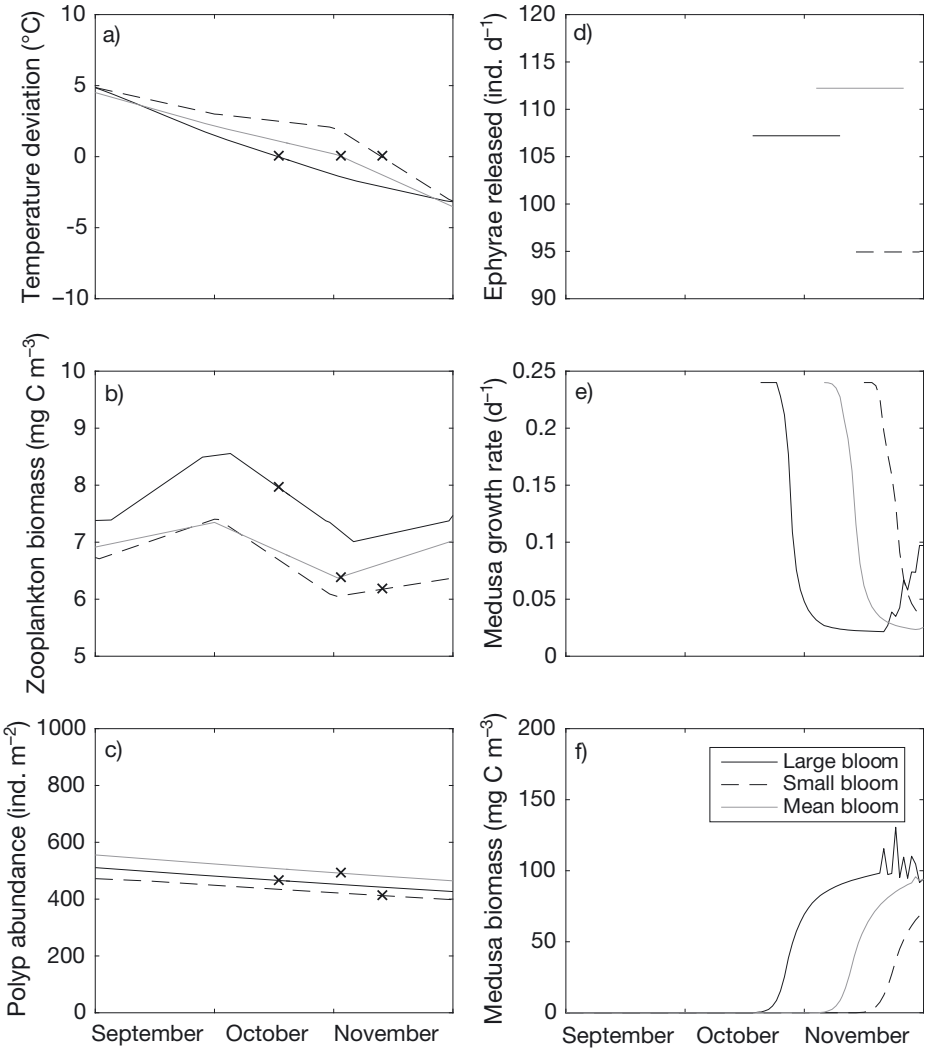

Fig. 7. Autumn time series of (a) temperature deviation, (b) zooplankton biomass, (c) polyp abundance, (d) ephyrae production, (e) medusa growth rate and (f) medusa biomass during large, small and mean medusa blooms. The large bloom is the mean of years 1993, 1995 and 1997; the small bloom is the mean of years 1988, 2002 and 2006; and the mean bloom is the mean of the whole time series (1982–2007). The initiation of strobilation (i.e. first release of ephyrae) is represented by the '×' symbols in panels a–c

when strobilation was initiated, particularly as the amount of ephyrae released per polyp increases with temperature until a peak at 20°C, before declining rapidly for both temperate and tropical species (Fig. 3b; Pascual et al. 2015). H_1 strobilation temperatures (<20°C) therefore would have resulted in a higher fraction of polyps reproducing and more ephyrae released per polyp compared to warmer temperatures in H_2 and H_3 (>20°C). As there was no relationship between polyp abundance and medusa biomass, this suggests that polyp-carrying capacity only influences the overall magnitude of a medusa bloom, but not inter-annual variations in biomass. Thus, if applying this model to other locations, it will be necessary to calibrate the polyp-carrying capacity to match the observed magnitude of jellyfish blooms. Other additional parameterization and/or structural adjustments may be necessary to successfully apply this model to other locations; however, the extent of these adjustments can only be fully assessed by testing the model in these locations, which is beyond the scope of this study.

Medusa community dynamics

The initiation of strobilation has been assessed in laboratory experiments, but rarely in the field, and the mechanistic driver behind when polyps strobilate is still unknown. This has been made more difficult

since the timing and frequency of ephyrae release varies across species, locations and years (Lucas 2001, Purcell et al. 2009). While it is well established that temperature changes can induce polyp strobilation in the laboratory (Purcell et al. 2009, 2012), the initiation of strobilation has also been observed to occur prior to the upcoming bloom of zooplankton (Willcox et al. 2008)—possibly as a way to ensure increased survival and fitness for the ephyrae. In our model, the best strobilation hypotheses to simulate the autumnal bloom of *Aurelia* spp. corresponded with the annual zooplankton minima (H_2 and H_3) instead of the annual temperature minima (H_1). While both H_2 and H_3 could reproduce the observed seasonal variation in medusa biomass, the later strobilation in H_3 could more appropriately reproduce the inter-annual variations in medusa biomass that were observed in the SEAMAP data trawls. The apparent dependence on zooplankton bloom timing shown here does not negate a temperature dependence of strobilation, but does negate a dependence on the temperature minimum. The autumnal blooms of *Aurelia* spp. in the Gulf of Mexico could be dependent on the rate of temperature decline from the summer peak, with maximum declines in temperature occurring approximately around H_3 (Fig. 2). Another scyphozoan, *Chrysaora* sp., regularly blooms during summer in the Gulf of Mexico (Robinson & Graham 2013), which would coincide with strobilation occurring around the temperature minimum (H_1). As *Chrysaora* sp. has been observed to prey on *A. aurita* in the laboratory (Sato et al. 1996, Kinoshita et al. 2006), this suggests that the later autumnal bloom for *Aurelia* spp. in the Gulf of Mexico may have developed as a response to minimize competition and/or predation. Determining the exact environmental cues for the initiation of strobilation, and the amount of strobilation events per year, will be necessary to correctly predict and forecast medusa populations in other locations.

In the Gulf of Mexico, higher abundances of jellyfish were observed during years when there was a cooler than average spring and warmer than average summer and autumn, leading Robinson & Graham (2013) to suggest that biophysical factors affecting polyp and ephyrae production determined the resulting medusa biomass. This is based on laboratory and *in situ* studies which have identified that the fraction of polyps strobilating and the amount and rate of ephyra release increase with increasing temperature, zooplankton biomass and light exposure (Lucas 2001, Purcell et al. 2009, 2012). Larger blooms of medusa biomass in the H_3 simulation were explained by higher zooplankton biomass prior to and at the initiation of strobilation and lower temperature deviation from where $Pulse_{max}$ occurs after strobilation (Table 4; Fig. 7). Higher zooplankton biomass at and before strobilation led to higher polyp ingestion rates, which allowed more carbon to be stored for ephyrae production. This resulted in higher numbers of ephyrae being released after strobilation was initiated. A lower temperature deviation from the optimum resulted in higher pulsation rates, resulting in higher ingestion and therefore growth rates, of the newly released ephyrae. Additionally, earlier bloom initiation resulted in larger blooms occurring during the autumn sampling period, whereas in the small bloom years medusa biomass peaked during winter. It is unclear whether medusa blooms in the Gulf of Mexico continue to exist in winter as there are no samples to compare against. It is possible that increased dispersion of individuals due to strengthening winter winds and currents (Muller-Karger et al. 2015) may result in higher medusa mortality during winter. However, this model does not currently parameterize mortality as a result of wind stress, and therefore it is still unknown whether a winter bloom terminates more rapidly than an autumn bloom. Regardless, the higher autumnal medusa biomass observed during the 1990s in the Gulf of Mexico was likely a result of earlier strobilation and more ideal environmental conditions around the time of strobilation which allowed for increased ephyrae production and ephyrae growth rates, consistent with the hypothesis of Robinson & Graham (2013).

Model limitations

Parameters chosen in this model fall well within empirical ranges and compare well with those chosen in previous dynamic scyphozoan population models (Xie et al. 2015). However, due to a lack of laboratory or observational data, there remains significant uncertainty around jellyfish population dynamics. In order to overcome this, this model was designed as an initial mechanistic framework to explore this uncertainty and the assumptions that were required to parameterize the model. Only a few studies have investigated the dynamics of scyphozoan polyp communities *in situ*, hence both the timing of strobilation initiation and the polyp-carrying capacity had to be determined through best guess estimates (Table 1). In this model, polyp-carrying capacity was calibrated within its broad range to recreate observed medusa biomass, and strobilation

time was tested with the alternative strobilation hypotheses to determine the best fit for this region. Despite their uncertainty, given adequate observations to compare against, a similar method can be used to calibrate these parameters to fit across other locations.

Another factor that remains relatively uncertain in the model is the timing of sexual maturity in female medusae. There appears to be no clear relationship between size or age of females and sexual maturity, with the size of maturity ranging from 19 to 310 mm (Lucas 2001). The size at which females mature sexually will influence the amount of planulae larvae produced (Lucas 1996) and the longevity of the medusa bloom, since post-reproductive medusae are believed to shed their feeding organs during reproduction, resulting in starvation (Spangenberg 1965, Möller 1980). Based on our sensitivity analysis, variations in the timing of female maturity had a negligible influence on the timing, magnitude or inter-annual variation of the medusa bloom despite the higher mortality rates for senescent medusae. As bloom demise in the field is observed to be quite rapid, we believe that there is less uncertainty around this mortality rate compared to the timing of female maturity. Nonetheless, future empirical work should examine the relationship between the size and timing of sexual maturity with environmental variables, as well as the rate of post-reproductive mortality in order to improve our understanding of medusa bloom longevity and demise.

Concluding remarks

Insufficient long-term jellyfish abundance data and knowledge of polyp community dynamics limits our predictive capabilities in determining how jellyfish communities will respond to climate change. This model enabled an analysis of different strobilation hypotheses to determine which hypothesis could successfully recreate the seasonal and inter-annual bloom dynamics of *Aurelia* spp. in the Gulf of Mexico. The magnitude of the medusa bloom was strongly regulated by the density of the polyp community, whereas its seasonality and inter-annual variation were influenced by the timing and environmental conditions at the initiation of strobilation. Increased zooplankton biomass and warmer temperatures around the initiation of strobilation resulted in larger blooms of medusae in the Gulf of Mexico, suggesting that this model may be able to predict large bloom years if coupled with a hydrodynamic model of the area. As polyp and ephyrae community dynamics were an integral driver of medusa blooms, in order to make accurate assessments of bloom dynamics, these life stages need to be explicitly included in future studies. To improve the predictive capabilities of this model, future research should prioritize the analysis of polyp community dynamics *in situ*, including density-dependent relationships and environmental drivers of strobilation, as well as improving our understanding of factors that contribute to bloom demise. The ability to predict variations in medusa bloom magnitude will inform management practices in the short term, and increase our understanding of how jellyfish communities will respond to long-term changes.

Acknowledgements. This is a product of the Nippon Foundation Nereus Program, a collaborative initiative by the Nippon Foundation and partners including Princeton University. We thank C. Petrik and D. Tommasi for comments on the manuscript. Images in Fig. 1 were drawn by A. FitzMaurice.

LITERATURE CITED

Agassiz L (1860) Contribution to the natural history of the United States of America. Little, Brown & Company, Boston

Arai MN (1997) A functional biology of Scyphozoa. Chapman & Hall, London

Arai MN (2009) The potential importance of podocysts to the formation of scyphozoan blooms: a review. Hydrobiologia 616:241–246

Burke WD (1975) Pelagic cnidaria of Mississippi Sound and adjacent waters. Gulf Res Rep 5:23–38

Burke WD (1976) Biology and distribution of the macrocoelenterates of Mississippi Sound and adjacent waters. Gulf Res Rep 5:17–28

Ceh J, Gonzalez J, Pacheco AS, Riascos JM (2015) The elusive life cycle of scyphozoan jellyfish—metagenesis revisted. Sci Rep 5:12037

Coyne JA (1973) An investigation of the dynamics of population growth and control in scyphistomae of the scyphozoan *Aurelia aurita.* Chesap Sci 14:55–58

Dawson MN, Martin LE (2001) Geographic variation and ecological adaptation in *Aurelia* (Scyphozoa, Semaeo stomeae): some implications from molecular phylogenetics. Hydrobiologia 451:259–273

Decker MB, Brown CW, Hood RR, Purcell JE and others (2007) Predicting the distribution of the scyphomedusa *Chrysaora quinquecirrha* in Chesapeake Bay. Mar Ecol Prog Ser 329:99–113

Di Camillo CG, Betti F, Bo M, Martinelli M, Puce S, Bavestrello G (2010) Contribution to the understanding of seasonal cycle of *Aurelia aurita* (Cnidaria: Scyphozoa) scyphopolyps in the northern Adriatic Sea. J Mar Biol Assoc UK 90:1105–1110

Fu Z, Shibata M, Makabe R, Ikeda H, Uye S (2014) Body size reduction under starvation, and the point of no return, in ephyrae of the moon jellyfish *Aurelia aurita.* Mar Ecol Prog Ser 510:255–263

Fuchs B, Wang W, Graspeuntner S, Li Y and others (2014)

Regulation of polyp-to-jellyfish transition in *Aurelia aurita.* Curr Biol 24:263–273
Gambill M, Peck MA (2014) Respiration rates of the polyps of four jellyfish species: potential thermal triggers and limits. J Exp Mar Biol Ecol 459:17–22
Gatz AJ Jr, Kennedy VS, Mihursky JA (1973) Effects on temperature on activity and mortality of the scyphozoan medusa, *Chrysaora quinquecirrha.* Chesap Sci 14:171–180
Gershwin L, Condie SA, Mansbridge JV, Richardson AJ (2014) Dangerous jellyfish blooms are predictable. J R Soc Interface 11:20131168
Graham WM (2001) Numerical increases and distributional shifts of *Chrysaora quinquecirrha* (Desor) and *Aurelia aurita* (Linné) (Cnidaria: Scyphozoa) in the northern Gulf of Mexico. Hydrobiologia 451:97–111
Graham WM, Pagès F, Hamner WM (2001) A physical context for gelatinous zooplankton aggregations: a review. Hydrobiologia 451:199–212
Gröndahl F (1988) Interactions between polyps of *Aurelia aurita* and planktonic larvae of scyphozoans: an experimental study. Mar Ecol Prog Ser 45:87–93
Hamner WM, Dawson MN (2009) A review and synthesis on the systematics and evolution of jellyfish blooms: advantageous aggregations and adaptive assemblages. Hydrobiologia 616:161–191
Hamner WM, Jenssen RM (1974) Growth, degrowth, and irreversible cell differentiation in *Aurelia aurita.* Am Zool 14:833–849
Han C, Uye S (2010) Combined effects of food supply and temperature on asexual reproduction and somatic growth of polyps of the common jellyfish *Aurelia aurita* s.l. Plankton Benthos Res 5:98–105
Han C, Chae J, Jin J, Yoon W (2012) Estimation of the minimum food requirement using the respiration rate of medusa of *Aurelia aurita* in Sihwa Lake. Ocean Sci J 47: 155–160
Haraldsson M, Tönnesson K, Tiselius P, Thingstad TF, Aksnes DL (2012) Relationship between fish and jellyfish as a function of eutrophication and water clarity. Mar Ecol Prog Ser 471:73–85
He J, Zheng L, Zhang W, Lin Y (2015) Life cycle reversal in *Aurelia* sp. 1 (Cnidaria, Scyphozoa). PLOS ONE 10: e0145314
Holling CS (1966) The functional response of invertebrate predators to prey density. Mem Entomol Soc Can 98:5–86
Holst S (2012) Effects of climate warming on strobilation and ephyra production of North Sea scyphozoan jellyfish. Hydrobiologia 690:127–140
Holst S, Jarms G (2010) Effects of low salinity on settlement and strobilation of Scyphozoa (Cnidaria): Is the lion's mane *Cyanea capillata* (L.) able to reproduce in the brackish Baltic Sea? Hydrobiologia 645:53–68
Houghton JDR, Doyle TK, Wilson MW, Davenport J, Hays GC (2006) Jellyfish aggregations and leatherback turtle foraging patterns in a temperate coastal environment. Ecology 87:1967–1972
Ishii H, Bamstedt U (1998) Food regulation of growth and maturation in a natural population of *Aurelia aurita* (L.). J Plankton Res 20:805–816
Ishii H, Katsukoshi K (2010) Seasonal and vertical distribution of *Aurelia aurita* polyps on a pylon in the innermost part of Tokyo Bay. J Oceanogr 66:329–336
Ishii H, Watanabe T (2003) Experimental study of growth and asexual reproduction in *Aurelia aurita* polyps. Sessile Org 20:69–73
Kamiyama T (2011) Planktonic ciliates as a food source for the scyphozoan *Aurelia aurita* (s.l.): feeding activity and assimilation of the polyp stage. J Exp Mar Biol Ecol 407: 207–215
Kinoshita J, Hiromi J, Yamada Y (2006) Abundance and biomass of scyphomedusae, *Aurelia aurita* and *Chrysaora melanaster,* and ctenophora, *Bolinopsis mikado,* with estimates of their feeding impact on zooplankton in Tokyo Bay, Japan. J Oceanogr 62:607–615
Liu W, Lo W, Purcell JE, Chang H (2009) Effects of temperature and light intensity on asexual reproduction of the scyphozoan, *Aurelia aurita* (L.) in Taiwan. Hydrobiologia 616:247–258
Lucas CH (1996) Population dynamics of *Aurelia aurita* (Scyphozoa) from an isolated brackish lake, with particular reference to sexual reproduction. J Plankton Res 18: 987–1007
Lucas CH (2001) Reproduction and life history strategies of the common jellyfish, *Aurelia aurita,* in relation to its ambient environment. Hydrobiologia 451:229–246
Lucas CH, Graham WM, Widmer C (2012) Jellyfish life histories: the role of polyps in forming and maintaining scyphomedusa populations. Adv Mar Biol 63:133–196
Lucas CH, Jones DOB, Hollyhead CJ, Condon RH and others (2014) Gelatinous zooplankton biomass in the global oceans: geographic variation and environmental drivers. Global Ecol Biogeogr 23:701–714
Lynam CP, Gibbons MJ, Axelsen BE, Sparks CAJ, Coetzee J, Heywood BG, Brierley AS (2006) Jellyfish overtake fish in a heavily fished ecosystem. Curr Biol 16:R492–R493
Melica V, Invernizzi S, Caristi G (2014) Logistic density-dependent growth of an *Aurelia aurita* polyps population. Ecol Model 291:1–5
Miyake H, Terazaki M, Kakinuma Y (2002) On the polyps of the common jellyfish *Aurelia aurita* in Kagoshima Bay. J Oceanogr 58:451–459
Möller H (1980) Population dynamics of *Aurelia aurita* medusae in Kiel Bight, Germany (FRG). Mar Biol 60:123–128
Møller LF, Riisgård HU (2007a) Feeding, bioenergetics and growth in the common jellyfish *Aurelia aurita* and two hydromedusae, *Sarsia tubulosa* and *Aequorea vitrina.* Mar Ecol Prog Ser 346:167–177
Møller LF, Riisgård HU (2007b) Population dynamics, growth and predation impact of the common jellyfish *Aurelia aurita* and two hydromedusae, *Sarsia tubulosa* and *Aequorea vitrina*, in Limfjorden (Denmark). Mar Ecol Prog Ser 346:153–165
Muller-Karger FE, Smith JP, Werner S, Chen R and others (2015) Natural variability of surface oceanographic conditions in the offshore Gulf of Mexico. Prog Oceanogr 134:54–76
Ohman MD, Runge JA, Durbin EG, Field DB, Niehoff B (2002) On birth and death in the sea. Hydrobiologia 480: 55–68
Olesen NJ, Frandsen K, Riisgård HU (1994) Population dynamics, growth and energetics of jellyfish *Aurelia aurita* in a shallow fjord. Mar Ecol Prog Ser 105:9–18
Oviatt CA, Kremer PM (1977) Predation on the ctenophore, *Mnemiopsis leidyi,* by butterfish, *Peprilus triacanthus,* in Narragansett Bay, Rhode Island. Chesap Sci 18:236–240
Pascual M, Fuentes V, Canepa A, Atienza D, Gili J, Purcell JE (2015) Temperature effects on asexual reproduction of the scyphozoan *Aurelia aurita* s.l.: differences between exotic (Baltic and Red Seas) and native (Mediterranean Sea) populations. Mar Ecol 36:994–1002

Phillips PJ (1971) The pelagic Cnidaria of the Gulf of Mexico 212. Texas A & M University, College Station, TX

Pitt KA (2000) Life history and settlement preferences of the edible jellyfish *Catostylus mosaicus* (Scyphozoa: Rhizostomeae). Mar Biol 136:269–279

Purcell JE (2007) Environmental effects on asexual reproduction rates of the scyphozoan *Aurelia labiata.* Mar Ecol Prog Ser 348:183–196

Purcell JE, Uye S, Lo W (2007) Anthropogenic causes of jellyfish blooms and their direct consequences for humans: a review. Mar Ecol Prog Ser 350:153–174

Purcell JE, Hoover RA, Schwarck NT (2009) Interannual variation of strobilation by the scyphozoan *Aurelia labiata* in relation to polyp density, temperature, salinity, and light conditions *in situ.* Mar Ecol Prog Ser 375:139–149

Purcell JE, Atienza D, Fuentes V, Olariaga A, Tilves U, Colahan C, Gili J (2012) Temperature effects on asexual reproduction rates of scyphozoan species from the northwest Mediterranean Sea. Hydrobiologia 690:169–180

Robinson KL, Graham WM (2013) Long-term change in the abundances of northern Gulf of Mexico scyphomedusae *Chrysaora* sp. and *Aurelia* spp. with links to climate variability. Limnol Oceanogr 58:235–253

Sato R, Hiromi J, Kadota S (1996) Interspecific relation between jellyfishes: laboratory observations of predation by the scyphomedusa *Chrysaora pacifica* upon *Aurelia aurita.* Jpn Bull Coll Agric Vet Med Nihon Univ 53:65–71

Schneider G (1989) Estimation of food demands of *Aurelia aurita* medusae populations in the Kiel Bight/Western Baltic. Ophelia 31:17–27

Spangenberg DB (1965) Cultivation of the life stages of *Aurelia aurita* under controlled conditions. J Exp Zool 159:303–318

Steele JH, Henderson EW (1993) The significance of interannual variability. In: Evans GT, Fasham MJR (eds) Towards a model of ocean biogeochemical processes. Springer, Berlin, p 237–260

Uye S, Shimauchi H (2005) Population biomass, feeding, respiration and growth rates, and carbon budget of the scyphomedusa *Aurelia aurita* in the Inland Sea of Japan. J Plankton Res 27:237–248

Watanabe T, Ishii H (2001) *In situ* estimation of ephyrae liberated from polyps of *Aurelia aurita* using settling plates in Tokyo Bay, Japan. Hydrobiologia 451:247–258

Willcox S, Moltschaniwskyj NA, Crawford CM (2008) Population dynamics of natural colonies of *Aurelia* sp. scyphistomae in Tasmania, Australia. Mar Biol 154: 661–670

Xie C, Fan M, Wang X, Chen M (2015) Dynamic model for life history of Scyphozoa. PLOS ONE 10:e0130669

Editorial responsibility: Verónica Fuentes (Guest Editor), Barcelona, Spain

Submitted: December 30, 2016; Accepted: July 10, 2017
Proofs received from author(s): September 5, 2017